INL/CON-14-32412
PREPRINT

Investigation of the Fission Products Silver, Palladium and Cadmium in Neutron Irradiated SiC using a Cs-Corrected HRTEM

Proceedings of the HTR 2014

I. J. van Rooyen, E. J. Olivier and J. H Neethling

October 2014

The INL is a
U.S. Department of Energy
National Laboratory
operated by
Battelle Energy Alliance

Proceedings of the HTR 2014
Weihai, China, October 27-31, 2014
Paper HTR2014-3-1255

Investigation of the Fission Products Silver, Palladium and Cadmium in Neutron Irradiated SiC using a Cs-Corrected HRTEM

I. J. van Rooyen[1], E. J. Olivier[2] and J. H Neethling[2]
[1]Fuel Performance and Design Department, Idaho National Laboratory
P.O. Box 1625, Idaho Falls ID, 83415-6188, USA
phone: +1-208-526-4199, isabella.vanrooyen@inl.gov

[2]Centre for High Resolution Electron Microscopy, Department of Physics,
Nelson Mandela Metropolitan University, Port Elizabeth, South Africa

Abstract – *Electron microscopy investigations of selected coated particles from the first advanced gas reactor experiment (AGR-1) at Idaho National Laboratory (INL) provided important information on fission product distribution and chemical composition in the SiC layer. Furthermore, recent STEM analyses led to the discovery of Ag at SiC grain boundaries and triple junctions. As these Ag precipitates were nano-sized, high resolution transmission electron microscopy (HRTEM) was used to provide more information at the atomic level. This paper describes some of the first HRTEM results obtained from the examination of a particle from Compact 4-1-1, which was irradiated to an average burnup of 19.38% fissions per initial metal atom (FIMA), a time-average, volume-averaged temperature of 1072°C; a time-average, peak temperature of 1182°C and an average fast fluence of $4.13x10^{21}$ n/cm$^{2.}$ Based on gamma-ray analysis, it is estimated that this particle may have released as much as 10% of its available Ag-110m inventory during irradiation. The HRTEM investigation focused on Ag, Pd, and Cd due to the interest in Ag transport mechanisms and possible correlation with Pd and Ag previously found. Additionally, Compact 4-1-1 contains fuel particles fabricated with a different fuel carrier gas composition and lower deposition temperatures for the SiC layer relative to the Baseline fabrication conditions, which are expected to reduce the concentration of SiC defects resulting from uranium dispersion. Pd, Ag, and Cd were found to co-exist in some of the SiC grain boundaries and triple junctions. This study confirmed the presence of Pd both at inter- and intragranular sites; in the latter case specifically at stacking faults. Small Ag precipitates were observed at a distance of about 6.5 microns from the inner PyC/SiC interface.*

I. INTRODUCTION

A detailed understanding of the silver transport mechanism in polycrystalline 3C-SiC is important for the design of advanced coated fuel particles for high temperature reactors. The finding, more than three decades years ago, that silver can be released by intact TRISO particles has led to significant research efforts to determine a silver transport mechanism in SiC, since out-of-reactor experiments did not reveal any significant silver migration in SiC. Numerous ^{110m}Ag transport mechanisms, such as grain boundary diffusion, surface diffusion or vapor transport through interconnected nano-pores or nano-cracks, Pd-assisted transport alongside grain boundaries, etc., have been identified in these out-of-pile experiments [1 – 10].

Neethling and co-workers [5-7] annealed polycrystalline SiC in contact with a Pd-Ag compound out-of–pile and reported that palladium significantly enhanced the transport of silver along grain boundaries in SiC. It was also reported that Ag or a Ag-Si compound did not penetrate polycrystalline 3C-SiC in the absence of Pd. Recent research by O'Connell and Neethling [10] reported enhanced Pd-Ag transport along grain boundaries in bulk (SiC grown by Rohm and Haas and irradiated at ORNL) neutron irradiated polycrystalline SiC annealed at 1000ºC (out-of–pile) compared to Pd-Ag transport in unirradiated SiC. In addition, Pd was also observed inside (at a distance of about 100 µm from the grain boundary) SiC grains of high fluence ($9.4x10^{21}$ n/cm^2 at 1460 ºC) irradiated samples. The neutron irradiation of SiC at high temperatures leads to the introduction of voids in rows along the {111} planes, which was found to enhance the transport of Pd in the SiC grains. Void formation is aided by the presence of lattice faults such as stacking faults and twins which readily form in SiC on {111} planes.

Although these individual studies are relevant to the specific experimental conditions, very few experimental results are reported to date on the fission product chemical composition and the location of Ag, and the transport in actual neutron irradiated SiC layers of TRISO coated particles which could be used to validate these out-of-pile hypotheses [11-13].

Therefore, the first direct measurement of silver in SiC grain boundaries of neutron irradiated TRISO coated particles from the first Advanced Gas Reactor (AGR-1) experiment by Van Rooyen and co-workers [13] provided a benchmark to confirm or to rule out some of these hypotheses. This work showed the co-existence of Ag and Cd in grain boundaries and triple points of the neutron irradiated SiC, Pd was found separately in different grain boundaries as well as inside the SiC grains. These results focused Idaho National Laboratory (INL) analytical electron microscopy investigation on Pd and Ag transport in SiC layers from TRISO coated particles.

In this paper analytical and high resolution STEM was used to examine the microstructure of and the location of fission products (Pd, Ag and Cd) in SiC irradiated to an average fast fluence of 4.13×10^{21} n/cm^2.

II. MATERIAL AND METHODS

II.A. Material

The initial results of the high resolution electron microscopy examination of a coated particle from Compact 4-1-1 from AGR-1 are described here. The unique compact identification number, 4-1-1 is based on the specific capsule, level, and stack number for each compact. Fig identifies the stack and position (or level) numbers in a particular capsule. Compact 4-1-1 refers to the compact in Capsule 4 at Level 1 of Stack 1. The capsule design and details of the AGR-1 experiment have been described previously [14].

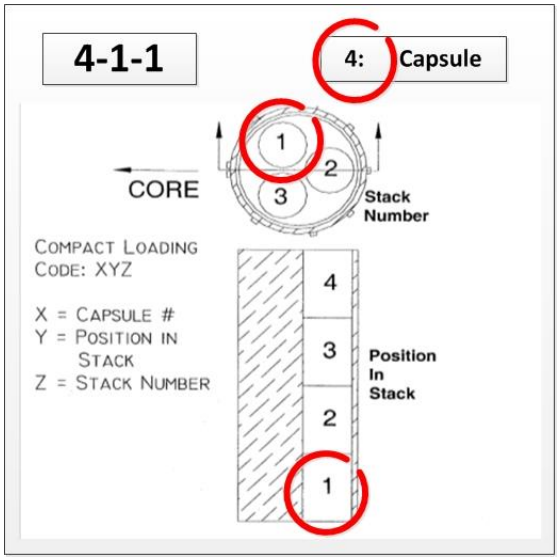

Fig 1. Numbering scheme for AGR–1 Compact 4-1-1.

Compact 4-1-1 contains Variant 3 fuel particles fabricated where the fuel carrier gas composition for the SiC layer vapor deposition was changed from 100% hydrogen to a 50% argon, 50% hydrogen mixture and the deposition temperature was lowered relative to the baseline (from 1500 to 1425°C). This change was expected to reduce the potential for SiC defects resulting from uranium dispersion and provide a variation in SiC microstructure that may be less permeable to metallic fission products. The fuel kernel is fabricated of low-enriched UCO (uranium oxycarbide) with a diameter of approximately 350 µm and U-235 enrichment of approximately 19.7%. Selected properties for the Variant 3 AGR-1 coated particles are shown in Table 1 [15].

Table 1. Selected properties (Actual Mean Value ± Population Standard Deviation) for the AGR-1 variant 3 coated particles [15].

Coating Layer	Mean value ± population standard deviation	
	Thickness (µm)	Density (mg/m^3)
Buffer	104.2 ± 7.8	1.10 ± 0.04
IPyC	38.8 ± 2.1	1.904 ± 0.013
SiC	35.9 ± 2.1	3.205 ± 0.001
OPyC	39.3 ± 2.1	1.911 ± 0.008

Compact 4-1-1 was irradiated to 19.38% fissions per initial metal atom (FIMA) average burnup, 1072°C time-average, volume–averaged temperature; 1182°C time-average, peak temperature

and an average fast fluence of 4.13×10^{21} n/cm^2. Individual particles were gamma-ray counted to measure the activity of various gamma ray emitting fission products. The retention of ^{110m}Ag in each particle is estimated by comparing the measured inventory to the predicted inventory normalized by the relative Cs-137 activity to reduce the influence of different kernel sizes on the overall distribution (see [15] for details).

The measured-to-calculated ratio for 58 gamma ray counted particles from Compact 4 ranged from 0.075 to 1.45. Coated particle AGR1-411-030 was selected because it exhibited an average retention of ^{110m}Ag under irradiation with the measured-to-calculated ^{110m}Ag ratio of 0.90 (Fig. 2). Deconsolidation-leach-burn-leach (DLBL) data [15] indicates that the particles from Compact 4-1-1 released on average approximately 3% of their inventory during the irradiation which was then retained in the matrix. It is concluded that on average there was relatively low release of silver from the particles in this compact. Decay corrected activity (in Bq) for Ag-110m measured by gamma ray counting of AGR1-411-030 particle is 6.45 x 10^4 [15].

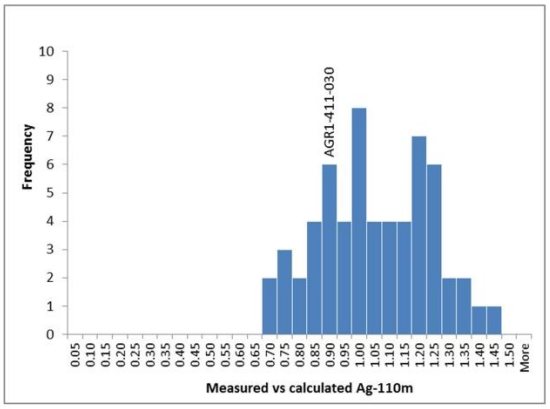

Fig 2. Distribution of measured-to calculated Ag-110m activity ratios, normalized by the Cs-137 activity to account for variations in fissile content and burnup.

II.B Methods

The specimens were prepared at the Electron Microscopy Laboratory (EML) at the Materials and Fuels Complex (MFC) of INL using the dual-beam Quanta 3D FEG focused ion beam (FIB) (Fig. 3). FIB lamellas at position 1b, 1c and 2 were extracted from locations perpendicular to the SiC-IPyC interface. Lamellas 1b and 2 contain parts of both the IPyC and SiC layers while FIB lamella 1c is from the outer interface between the SiC and OPyC layer, the furthest away from the IPyC-SiC interface. FIB lamella 1a contained only a small area of the SiC layer close to the IPyC-SiC interface, and was cut parallel to the IPyC-SiC interface. As lamella 1a contained only small areas of the SiC layer at the IPyC-SiC interface, it was not examined for this paper.

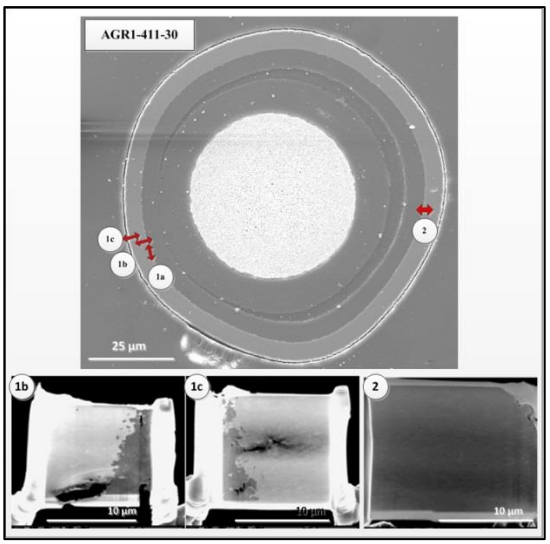

Fig. 3. SEM image showing the AGR1-411-030 FIB-SEM lamellas sectioned at positions 1b, 1c and 2 as indicated on the cross-section of the coated particle.

HRTEM and HRSTEM investigations were performed at the Nelson Mandela Metropolitan University (NMMU) in South Africa using a double Cs-corrected JEOL ARM 200F operated at 200 kV. This microscope is equipped with two CEOS spherical aberration (Cs) correctors for correction in TEM and STEM modes, as well as an Oxford Instruments XMAX 80 electron dispersive spectroscopy (EDS) detector and Gatan Quantum Image filter with dual electron energy loss spectroscopy (EELS) capabilities.

Imaging and analysis of the sample were done using a sub-angstrom sized probe with a probe current of approximately 68 pA, which was found to give the best balance of resolution, count rate and sample stability. EDS was mainly used for compositional analysis due to the relative accessibility of the higher energy K-lines for Ag and Pd which enabled their easy identification due to sufficient separation between the respective X-ray peaks. Another distinct advantage of the microscope is that of the simultaneous acquisition of both bright field (BF) and high angle annular dark field (HAADF) STEM images. This aided in the identification of grain boundaries in conjunction with elemental atomic number contrast imaging. The main objective of this investigation was to obtain very high resolution images of the fission products and their surroundings.

II.C. HRSTEM Investigation and Approach

The Cs-corrected HRTEM was operated in scanning transmission mode which allows for simultaneous viewing of BF and HAADF STEM

images. This mode of viewing enables the easy differentiation between SiC and PyC areas as well as the identification of fission product agglomerates in the form of nodules inside the SiC layer. The BF image provides sufficient contrast to identify the positions of grain boundaries as well as the presence of defects such as stacking faults, which can then be correlated with the position of fission products by using the HAADF imaging, which shows atomic number (Z) contrast. After HRSTEM imaging of the sites containing visible fission product agglomerates, EDS spot analysis was carried out on the fission products and surrounding areas to identify the elements present. Probe current conditions were chosen to optimize the beam current but at the same time minimize beam damage to the specimen.

III. RESULTS AND DISCUSSION

III. A. SiC as main barrier to fission products

The effectiveness of the SiC layer as the main fission product barrier is illustrated by the HAADF STEM images in Fig.4 where the accumulation of Pd at the IPyC-SiC interface is visible. Additionally, no significant Pd corrosion of SiC, only a few ~ 1 nm diameter corrosion pits is observed even at this high magnification, which confirms earlier SEM observations and proves that Pd can penetrate the SiC without corroding the surface significantly [11].

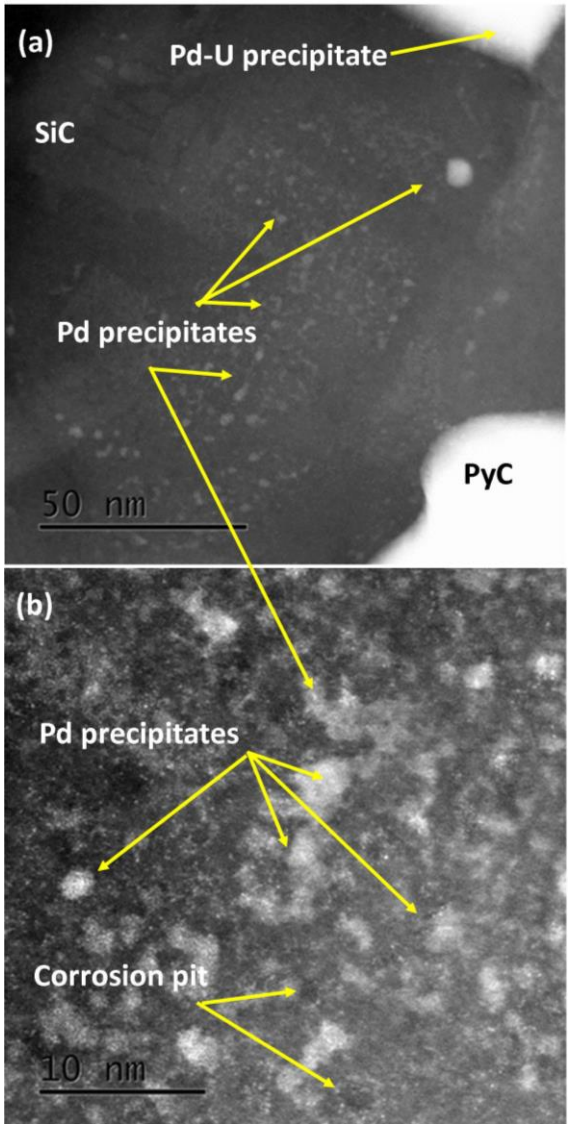

Fig. 4. HAADF STEM images showing (a) the accumulation of Pd at the IPyC-SiC interface, and (b) showing no significant corrosion except for a few ~ 1 nm diameter corrosion pits only visible at this magnification.

III.B. Co-existence of Ag, Pd and Cd at grain boundaries and triple junctions

BF and HAADF STEM images of fission product networks at SiC grain boundaries and triple points of specimen AGR-411-030 position 1b are shown in Fig. 5 (a) and (b) respectively. These fission product accumulations are visible as bright regions (high atomic number) in the HAADF STEM shown in Fig. 5 (b). Accumulations of Pd, Ag and Cd were found to co-exist in the area indicated by arrow marked 1 in the HAADF STEM image (b). The arrowed area 1 in Fig. 5(b) is shown at higher magnification in Fig. 6 as a BF STEM image of co-existing Pd-Ag-Cd accumulations at location 1 on a grain boundary between two SiC grains. Fig. 7 shows the EDS

spectrum at location 1 in Fig. 6. EDS analyses of locations 2 and 3 only indicated the presence of Pd. However, the possible presence of Ag or Cd at locations 2 or 3 in concentrations below the EDS detection limit cannot be ruled out.

Under certain imaging conditions, HAADF and BF STEM images are complementary and therefore the atom columns in DF mode will change from bright spots to dark spots in BF mode. The dark spots at the grain boundary and at the triple points in Fig. 6 are therefore due to the Pd, Ag or Cd atoms. It is not possible to differentiate between these elements using BF STEM imaging. The EDS analyses caused the slight damage to the atomic structure visible at the locations arrowed in Fig. 6.

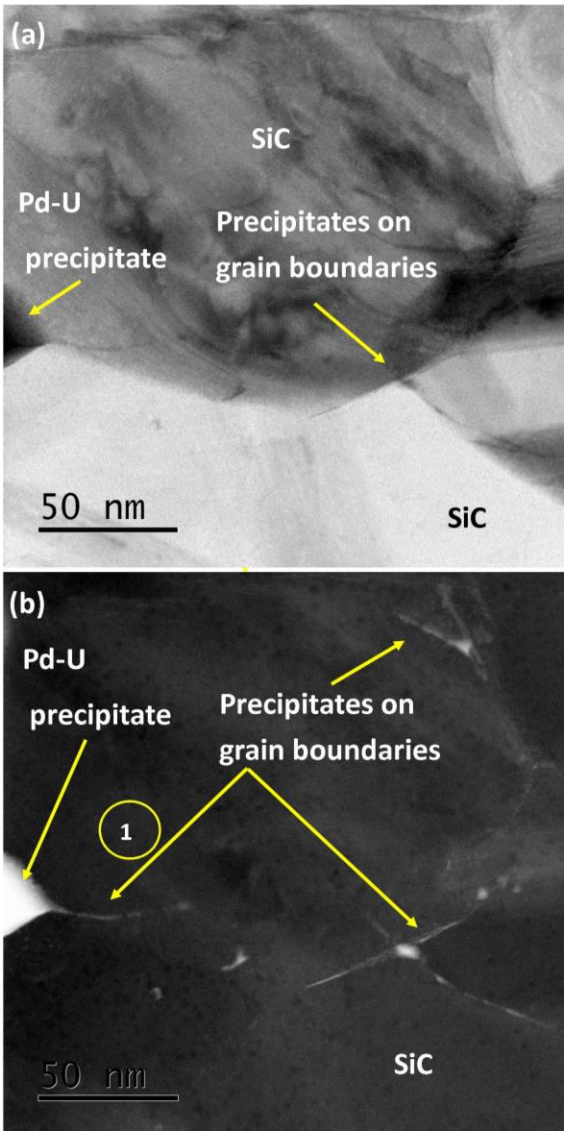

Fig. 5. Bright field ((a) and dark field (b) STEM images of fission product networks at grain boundaries and triple points of specimen AGR-411-030 position 1b .

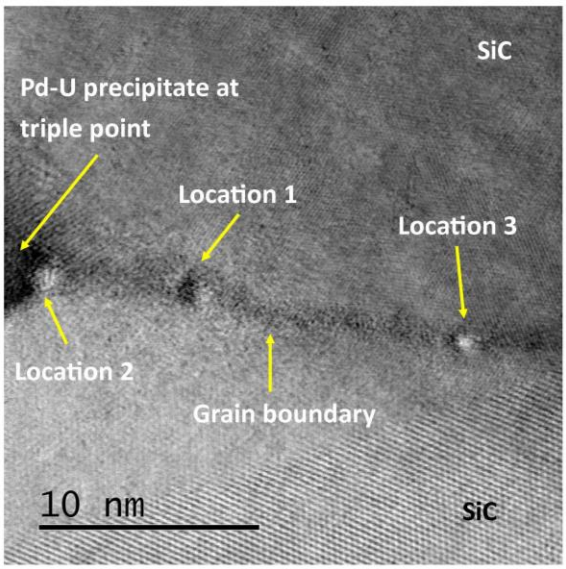

Fig. 6. High resolution BF STEM image Pd-Ag-Cd accumulations co-existing at location 1 at a SiC grain boundary of specimen AGR-411-030 position 1b. Only Pd was found at locations 2 and 3.

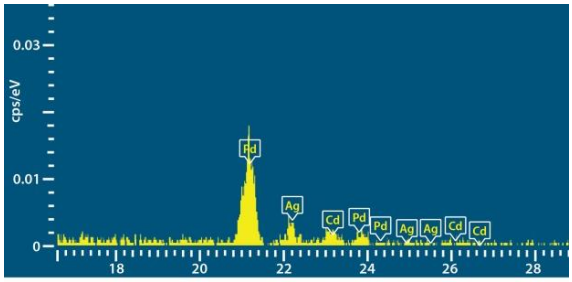

Fig. 7 EDS spectrum showing co-existence of Pd, Ag and Cd at location 1, Fig. 6, of specimen AGR-411-030 position 1b.

The accumulations of Pd, Ag, and Cd co-existing in other areas of specimen AGR-411-030 position 1b, was also confirmed by the HAADF STEM image shown in Fig. 8 with the corresponding EDS spectrum in Fig. 9. Only Pd was found in nearby "larger" triple point accumulations as shown in Fig. 9. Higher magnification BF STEM images of the Pd-Ag-Cd containing triple point are shown in Fig 10. In the BF STEM image the atoms are visible as dark spots at the grain boundary and the triple point, as well as deeper into the SiC grain. As was mentioned before, it is not possible to differentiate between the elements using BF STEM.

It is suggested that Ag decay is most likely the primary source of the Cd observed in the fission product nodules. It is therefore to be expected that at the end of the irradiations, Cd will be present in close proximity to Ag. However, Cd is also a direct fission product (albeit one of lower yield and higher vapor pressure compared with Ag and Pd) and it is

therefore possible that some of the Cd observed could have been created by fission.

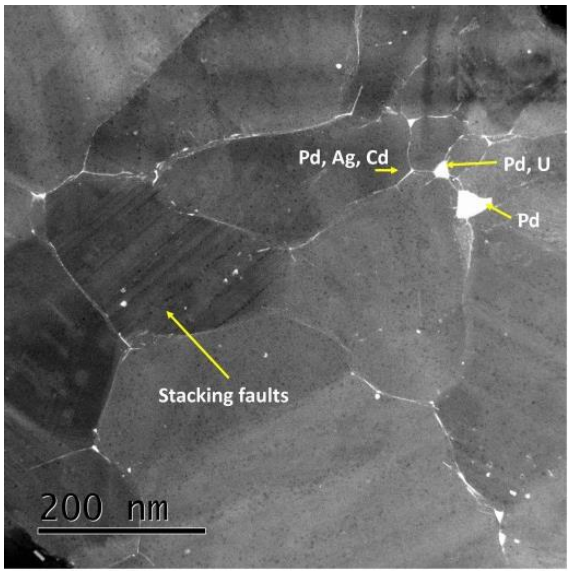

Fig. 8. HAADF STEM image of specimen AGR-411-030 position 1b, showing a triple point where Pd, Ag, and Cd accumulations co-exist, Only Pd was found in nearby "larger" triple point accumulations.

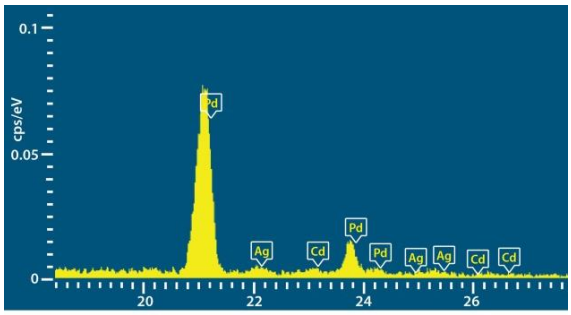

Fig. 9. Corresponding EDS spectrum showing the co-existence of Pd, Ag, and Cd in a second area of specimen AGR-411-030 position 1b.

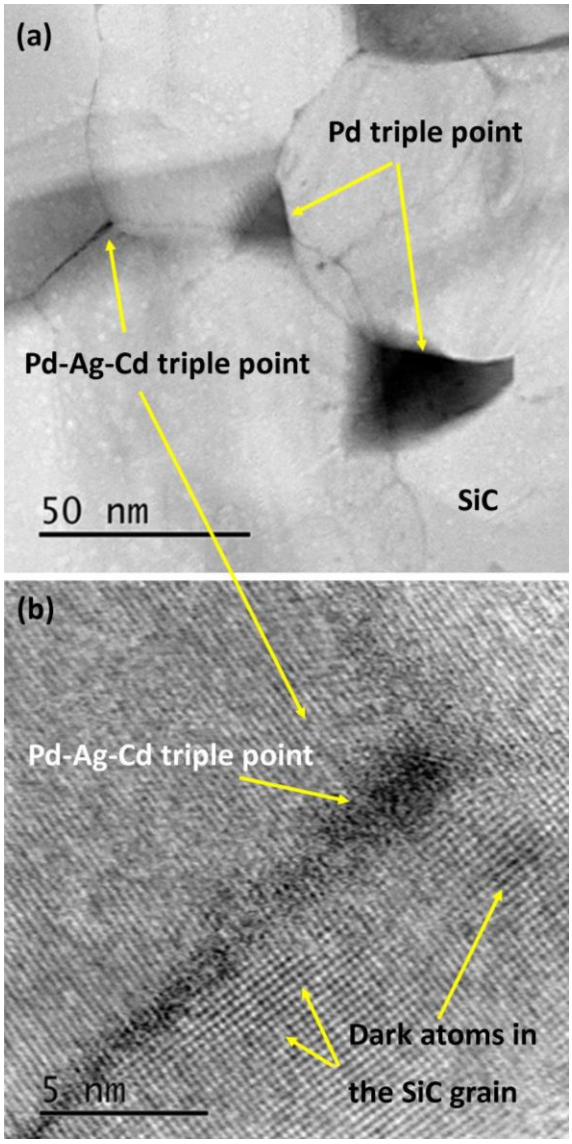

Fig. 10. BF STEM image (a) of a Pd-Ag-Cd containing triple point with the corresponding high resolution BF STEM image (b) with atoms visible as dark spots are also visible deeper into the SiC grain.

III.C. Intragranular presence of Pd in SiC

Pd was also observed inside SiC grains in proximity to planar defects such as stacking faults or nano twins (see Fig. 11). This is an interesting observation since the majority of Pd nodules are usually found along SiC grain boundaries. However it is proposed that the same mechanism that governs the movement of Pd along SiC grain boundaries is responsible for the migration of Pd along planar defects in SiC. Grain boundaries contain high concentrations of dislocations due to the relative misorientation between adjacent grains and therefore have a comparatively open structure. This results in diffusivities for grain-boundary transport that are much larger than analogous values for lattice

diffusion. Enhanced diffusion along dislocation cores will also occur. SiC grains containing high concentrations of stacking faults (or nano-twins) bounded by partial dislocations will also have a high concentration of easy diffusion paths created by the stacking faults and partial dislocation cores. This is consistent with the work of Kornilios et al. [16] who suggested that the observed diffusion of gold through a 2.8 µm thick 3C-SiC layer at 500ºC for 500 h was most likely along stacking faults extending through the layer.

Furthermore, the transport of Pd in SiC is assumed to be mediated by a silicide formation mechanism at temperatures in the range of 1000ºC. At temperatures above the melting point of the silicide (about 980ºC for Pd/Si), Si atoms will diffuse into the Pd nodule via an exchange mechanism with Pd atoms, which will release more Pd atoms to penetrate the SiC and react with Si atoms at the grain's boundaries. It is for this reason that the migration of Pd is seen to occur preferentially along grain boundaries. As mentioned earlier, stacking faults and nano-twins also provide easy diffusion paths for atoms and may explain the presence of Pd at stacking faults (or nano-twins) inside the SiC grains observed in this study.

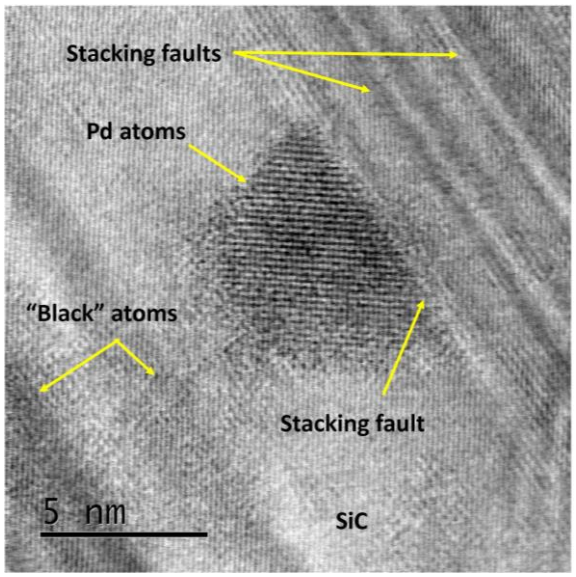

Fig. 11 High resolution BF STEM image of a Pd precipitate (Pd atoms visible as dark spots) which accumulated at a stacking fault in a SiC grain. Some dark spots are also visible in the SiC grain.

III.D. Penetration depth of fission products in the SiC layer

As significant Ag was released from this particle, it was our aim to identify locations of silver through the thickness of the SiC layer in an attempt to correlate the locations with local microstructure (e.g. grain size, grain boundary character). Thus, a lower limit for the penetration depth of Pd and Ag into SiC from the inner PyC/SiC interface was determined. The determination of the maximum penetration depth in SiC is challenging since the Pd nodules that are clearly visible at low magnification are not situated at the maximum penetration depth. When the magnification is increased, smaller hairline (~ 1 - 2 nm thick) networks of palladium become visible and extend further (frequently up to 8 µm) into the SiC than the larger nodules that are easily observed at lower magnification. EDS analyses of these hairline networks also become challenging when the concentration of Pd or Ag is of the same magnitude as the EDS detection limit. From this depth and deeper into the SiC, atomic migration along the grain boundaries, below the STEM and EDS detection limits, is possible and quite likely.

The Pd was found to be present in nodule networks throughout FIB lamellas 1b, 1c and 2. Ag was typically found within a 2 um zone from the inner PyC, but this could be due to the higher density of nodules present in this zone and the potential higher Ag content in this area. However, Ag is found at a distance of ~6.7 µm from the IPyC-SiC interface (Fig.12 and Fig.13 for higher magnification of this area) in this specific lamella and this value should be considered as a lower (detectable) limit for the current irradiation conditions of the TRISO particle and electron microscopy techniques employed for the investigation. It may however be stated with certainty that Ag has only been found together with Pd and Cd.

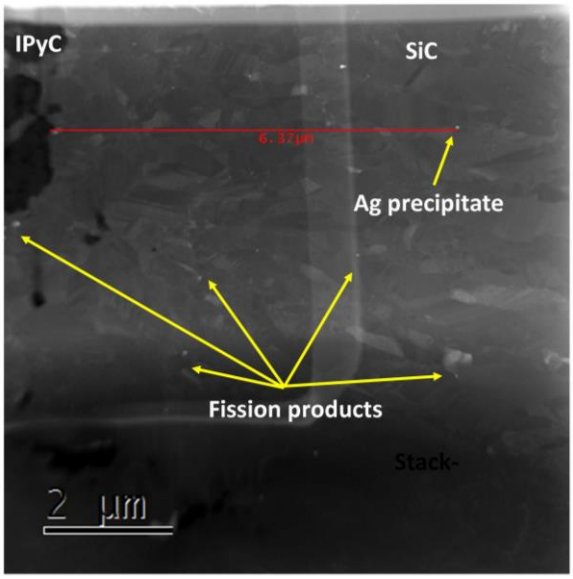

Fig. 12 BF STEM image of SiC showing the penetration depth of Ag measured in this specific SiC lamella.

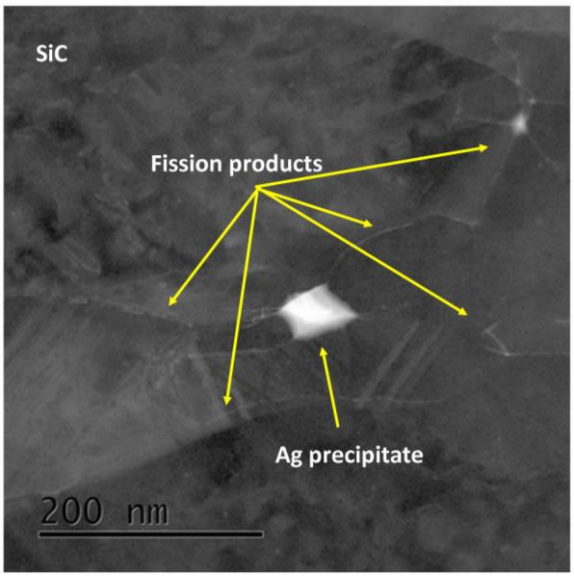

Fig 13 BF STEM image of SiC showing the penetration depth of Ag at higher magnification. At this larger magnification, more fission product tripple points are visible.

DISCUSSION AND CONCLUSIONS

This paper describes some of the first analytical HRSTEM results obtained from the examination of a particle from Compact 4-1-1, which was irradiated to an average burnup of 19.38% FIMA, a time average, volume-averaged temperature of 1072°C; a time average, peak temperature of 1182°C, and an average fast fluence of 4.13×10^{21} n/cm^2. Based on gamma-ray analysis, it is estimated that this particle may have released as much as 10% of its available Ag-110m inventory during irradiation.

It was observed by STEM imaging that Pd accumulated at the IPyC-SiC interface, which is an indication that Pd diffuses rapidly through the PyC layers until it reaches the SiC in which transport is much slower. This shows therefore the effectiveness of the SiC layer and the morphology of the IPyC/SiC interlayer as the main fission product barrier. Additionally, no significant Pd corrosion of SiC was observed, which confirmed earlier SEM observations and indicated that Pd can penetrate the SiC without corroding the surface significantly.

BF and HAADF STEM images of fission product networks at SiC grain boundaries and triple points of specimen AGR-411-030 indicated that accumulations of Pd, Ag and Cd co-existed at grain boundaries and triple points. At some locations, EDS analyses only indicated the presence of Pd. However, the possible presence of Ag or Cd at these locations in concentrations below the EDS detection limit cannot be ruled out. It is suggested that Ag decay is most likely the primary source of the Cd observed in the fission product nodules. It is therefore to be expected that at the end of the irradiations, Cd will be present in close proximity to Ag. If Cd accumulations were observed without any Ag, it could have indicated a source of Cd was fission in the kernel.

Pd was also observed inside SiC grains in proximity to planar defects such as stacking faults or nano twins. This is an interesting observation since the majority of Pd precipitates are usually found along SiC grain boundaries. However, previous STEM work by Van Rooyen et al [13] showed the presence of spherical nano Pd precipitates inside grains as well, but it was not possible to provide more positional information of these Pd precipitates inside the SiC grains. This HRTEM study therefore provides this new information and it is proposed that the same mechanism that governs the movement of Pd along SiC grain boundaries is responsible for the migration of Pd along planar defects in SiC. Grain boundaries contain high concentrations of dislocations due to the relative misorientation between adjacent grains and therefore have a comparatively open structure. This results in diffusivities for grain-boundary transport that are much larger than analogous values for lattice diffusion. Enhanced diffusion along dislocation cores will also occur. SiC grains containing high concentrations of stacking faults (or nano-twins) bounded by partial dislocations will also have a high concentration of easy diffusion paths created by the stacking faults and partial dislocation cores.

Furthermore, the transport of Pd in SiC is assumed to be mediated by a silicide formation mechanism at temperatures in the range of 1000ºC. At temperatures above the melting point of the silicide (~ 980ºC for Pd/Si), Si atoms will diffuse into the Pd nodule via an exchange mechanism with Pd atoms, which will release more Pd atoms to penetrate the SiC and react with Si atoms at the grain boundaries. It is for this reason that the migration of Pd is seen to occur preferentially along grain boundaries. As mentioned earlier, stacking faults and nano-twins also provide easy diffusion paths for atoms and may explain the presence of Pd at stacking faults (or nano-twins) inside the SiC grains observed in this study.

A lower limit for the penetration depth (~ 6.7 µm) of Pd and Ag into SiC from the inner PyC-SiC interface was determined. The determination of the maximum penetration depth in SiC is challenging since the Pd nodules that are clearly visible at low magnification are not situated at the maximum penetration depth. When the magnification is increased, smaller hairline networks of palladium becomes visible and it extends deeper (frequently up to 8 µm) into the SiC than the larger nodules that are easily observed at lower magnification. From this depth and deeper into the SiC, atomic migration

along the grain boundaries, below the STEM and EDS detection limits, is possible and quite likely.

It may however be stated with certainty that Ag has only been found together with Pd and Cd for samples from this specific compact and the current irradiation conditions. The finding that Ag has been found inside SiC at grain boundaries only in the presence of Pd, is consistent with the Pd assisted transport mechanism proposed by Neethling and co-workers [5]. This may also explain why the majority of the out-of-pile experiments carried out to determine the diffusion coefficient of Ag in SiC did not reveal any significant silver migration in SiC.

The fact that neutron irradiation was found to enhance the penetration rate of Pd in SiC along grain boundaries [10] is suggested to be a result of radiation damage and a corresponding increase in the point defect concentrations at the grain boundaries. Earlier work on irradiated TRISO coated particles [11] also revealed the alignment of voids at the grain boundaries in the vicinity of fission product precipitates.

Although the results of this analytical HRSTEM study are consistent with a Pd assisted Ag transport mechanism along grain boundaries, more research is needed to elucidate the effect of neutron irradiation damage (and irradiation temperature) on fission product transport at the nano- and atomic level, which is one of the research focus areas at INL.

ACKNOWLEDGEMENTS

This work was sponsored by the U.S. Department of Energy, Office of Nuclear Energy, under DOE Idaho Operations Office Contract DE-AC07-05ID14517. James Madden is acknowledged for the FIB sample preparation. David Petti, Paul Demkowicz and Jack Simonds are thanked for the review of this document. The Centre for HRTEM in South Africa gratefully acknowledged the financial support of the Department of Science and Technology, the National Research Foundation and Sasol.

REFERENCES

[1] H. Nabielek, P.E. Brown, P. Offerman, “Silver Release from Coated Particle Fuel”, Nucl. Techn. 35 (1977) 483.

[2] MacLean, H.J., Ballinger, R.G., Kolaya, L. E., Simonson, S.A., Lewis, N., Hanson, M.E., 2006. “The Effect of Annealing at 1500 ºC on Migration and Release of Ion Implanted Silver in CVD Silicon Carbide”, J. Nucl. Mater. 357, 31 – 47.

[3] Friedland, E., Malherbe, J.B., Van der Berg, N.G., Hlatshwayo, T., Botha, A.J., Wendler, E., Wesch, W., 2009. “Study of Diffusion in Silicon Carbide”, J. Nucl. Mater. 389, 326 - 331.

[4] E. Lopez, Honorato, D. X. Yang, J. Tan, P. J. Meadows, and P. Xiaow, “Silver Diffusion in Coated Fuel Particles,” J. Am. Ceram. Soc., 93 [10] 3076 3079 (2010).

[5] Olivier, E. J. and Neethling J. H., “Palladium Transport in SiC,” Nuclear Engineering and Design 244, 25-33 (2012)

[6] Neethling J. H., O’Connell J. H. and Olivier E. J., “Palladium Assisted Silver Transport in Polycrystalline SiC,” Nuclear Engineering and Design 251, 230-234 (2012)

[7] Olivier E. J. and Neethling J. .H, “The Role of Pd in the Transport of Ag in SiC”, Journal of Nuclear Materials, 432, 252-260 (2013)

[8] D. Schrader, S. M. Khalil, T. Gerzcak, T.R. Allen, A. J. Heim, I. Szlufarska, D. Morgan, “Ag Diffusion in Cubic Silicon Carbide”, J Nucl Mater, 408 (2011) 257-271

[9] S. Khalil, N. Swaminathan, D. Schrader, A. J. Heim, D.D. Morgan, I. Szlufarska, , “Diffusion of Ag Along Grain Boundaries in 3C-SiC”, Physical Review B 84, 214104 (2011)

[10] O’Connell, J.H. and Neethling J.H., “Ag Transport in High Temperature Neutron Irradiated 3C-SiC”, J. Nucl. Mater. 455, 20-25 (2014)

[11] I. J. van Rooyen, D. E. Janney, B. D. Miller, P. A. Demkowicz, J. Riesterer, “Electron Microscopic Evaluation and Fission Product Identification of Irradiated TRISO Coated Particles from the AGR-1 Experiment,” A Preliminary Review, Nuclear Engineering and design, 271 (2014) 114-122

[12] Paul A. Demkowicz, John D. Hunn, Scott A. Ploger, Robert N. Morris1, Charles A. Baldwin, Jason M. Harp, Philip L. Winston, Tyler Gerczak, Isabella J. van Rooyen, Fred C. Montgomery, Chinthaka M, Silva, “Irradiation Performance of AGR-1High Temperature Reactor Fuel,” Paper HTR2014-31182, Proceedings of the HTR 2014, Weihai, China, October 27-31, 2014

[13] I.J. van Rooyen T. M. Lillo, Y. Q. Wu, “Identification of Silver and Palladium in Irradiated TRISO Coated Particles of the AGR-1 Experiment,” Journal of Nuclear Materials 446 (2014) 178–186

[14] J. Maki, “AGR-1 Irradiation Experiment Test Plan”, INL/EXT-05-00593 rev. 3, 10/20/09.

[15] P. A. Demkowicz, J.M. Harp, P. L. Winston, S. A. Ploger, I. J. van Rooyen, B. D. Miller, J. Reisterer, “AGR-1 Compact 4-1-1 Post-Irradiation Examination”, Draft report

[16] N. Kornilios, G. Constantinidis, M. Kayiambaki, K. Zekentes and J. Stoemenos, “Diffusion of Gold in 3C-SiC Epitaxially Grown on Si: Structural Characterization” Mat. Sci. Eng. B46 (1997) 186 -189